1 Introduction: Why Cosmography?

The term cosmography was first coined by Humbolt in the late 1800s as an umbrella over the subsets of the descriptive astronomy, Uranography, and terrestrial mapping, or geography. Cosmography has been defined as the science of mapping or charting the world or the universe, but in the context of modern astrophysics, refers to making precision measurements of cosmological parameters. Cosmography measurements rely on this fundamental equation, relating the luminosity distance to the source to its redshift and the cosmological parameters:

$$D_L = \frac{c(1+z)}{H_0} \int_0^z \frac{dz'}{[\Omega_M(1+z')^3 + \Omega_\Lambda(1+z')^{3(1+\omega)}]^{1/2}} \tag{1}$$

where H_0 is the hubble constant, z is the redshift, c is the speed of light, Ω_M and Ω_Λ are the dimensionless matter density and dark energy density parameters of the universe, and ω determines the equation of state of dark matter. In the local universe, one can make measurements of the Hubble constant; the other cosmological parameters can only be constrained using sources from the high-redshift universe. In order to constrain the values of these cosmological parameters, one requires an independent measure of both the redshift and the luminosity distance to the source. One of the most popular methods involves using white dwarf supernovae as standardizable candles. The most viable model for creating such explosions, known as the doubly degenerate model, was hypothesized to occur when a merger of the white dwarfs exceeded the Chandrasekhar limit, and thereby had a standard intrinsic luminosity at merger. As such, by measuring the observed flux of the Type Ia supernovae, one could determine the distance to the source. More recent evidence suggests that that before using Type Ia supernovae as standard candles, one must correct for their lightcurves, which follow an established trend, and then calibrate the peak brightness using cepheid variable stars, one rung down from Type Ia supernovae in the cosmic distance ladder. The calibrated peak brightness would provide the distance to the source. Independently, one can determine the redshift of the source, using standard methods to analyze the SNe spectrum (C. Ngeow and S.M Kanbur, 2006). However, currently, such measurements face large systematic errors due to the fact that their progenitor composition is still largely a mystery (M. Sullivan et al., 2006). Using cosmographical measurements from Type Ia supernovae, astronomers determine H_0 to be 73 km/s/Mpc with a one percent errorbar (C. Ngeow and S.M Kanbur, 2006). However, recent measurements made by the Planck satellite determine the hubble parameter to be closer to 67 km/s/Mpc within two percent error. This secondary method employs the CMB power spectrum to determine the characteristic size scale of structure formation (baryon acoustic oscillation radius) and relate it to the redshift at which the CMB was released (z $\approx$ 1089). This large discrepancy regarding the acceleration rate of expansion of the local universe could be reconciled using gravitational wave cosmography. There are a few different proposed methods for performing cosmography using gravitational wave signals from both binary neutron star mergers and neutron star-black hole mergers. One such method involves a coincident short GRB observation with a BNS or NS-BH inspiral signal detection. Using the spectra of the optical counterpart of such an event, one can either determine redshift using spectral analysis, or localize the source to its host galaxy and thereby infer the source redshift from the galaxy's redshift. From the GW signal-to-noise ratio, one can find the distance independently, using the equation relating S/N to distance, D:

$$\rho \propto \frac{1}{D} \int_{f_2}^{f_1} \frac{f^{-\frac{7}{3}}}{S(f)} df \tag{2}$$

where ρ is the signal to noise ratio, S(f) is the noise as a function of frequency, $f^{-\frac{7}{3}}$ is the approximate scaling law of a BNS merger signal, and the expression is integrated from the lower bound of the frequency range the detector is sensitive to (20-30 Hz for Advanced LIGO) to the upper bound of the frequency at which the merger is expected to occur (this frequency is referred to as f_{ISCO}, which is a function of the masses of the sources in the system) (Singer et al., 2014). Because gravitational wave signals are well-modeled by numerical relativity, they are considered to be standard sirens, because we can obtain the distance to the source using its amplitude or S/N. Since the measures of redshift and distance described above are calibration-independent, compact binary coalesences have the potential of being used the same way as Type

Ia supernovae to measure distance scales (and the expansion rate) of the universe. Another method described in (Messenger et al., 2012) outlines a measurement of the redshift of the BNS or NS-BH merger by locating the signature of tidal disruption in the gravitational wave signal itself. Such a measurement would require a high enough signal-to-noise ratio to be able to easily distinguish from the noise. Currently, by assuming a cosmological model as well as values for the cosmological parameters in equation [1], one can infer the source-frame masses. However, if with next generation detectors we are able to tightly constrain the neutron equation of state, then, using the frequency at which tidal deformation occurs, one can break the degeneracy between mass and redshift, and thereby find both redshift and distance from the gravitational wave signal alone. An alternate method has been outlined in (Messenger et al., 2014) in which a typical BNS merger results in a hypermassive neutron star (HMNS) in the postmerger phase, that delays formation into a black hole, and has a unique signature in the gravitational wave signal that can beused to break the mass-redshift degeneracy. However, such studies are only possible with next generation detectors. The signal-to-noise ratios, as well as the sensitivities to distant sources are too low using second generation detectors; thus, this study, which will focus on the first two methods of cosmography with gravitational waves, involves networks of next generation detectors.

2 Goals

Due to the limited scope and time span of this two-month time period, we narrowed down this cosmography study to a few specific research questions we are interested in addressing. The overarching goal is to determine how well we can constrain the Hubble constant in the local universe using gravitional waves. In particular, our aim is to quantify the uncertainties in the redshifts and distance measures we expect to measure using these two methods, as well as the associated systematic biases with making those measurements. Some of the systematic biases we identify include:

• Malmquist bias - This bias occurs as a result of observing only the brightest sources in the sky, and neglecting to observe sources that are dimmer. This is the most likely explanation for why the number of gamma-ray bursts we observe at low flux is far less as compared to the theoretical flux distribution of gamma ray bursts (BATSE data).

• Distance/inclination angle degeneracy - Similar to the mass-redshift degeneracy, due to the fact that we determine the distance to the source from the signal-to-noise ratio of the signal, it is difficult to tell whether the loudness of the signal is directly due to the distance to the source, D, or the source inclination angle, ι (discussed below). Such a bias will affect our ability to accurately measure the source's distance from Earth.

• Face-on binary selection effect - Due to the gravitational wave antenna patterns that present interferometers are sensitive to, we anticipate there to be a bias towards measuring more face-on ($\iota = \pi/2$), rather than edge-on ($\iota = 0$) binary systems, due to the fact that face-on binaries produce detectable plus and cross polarization patterns. Similarly, the detector is more likely to detect sources that are directly overhead, as compared to sources closer the the horizon between the two detectors.

• Neutron star equation-of-state - While in the first cosmography method, we can treat the neutron stars as point masses since the redshift measurement comes from EM spectra, in order to determine the redshift from the tidal disruption frequency, we must assume a neutron star equation of state. There have been several proposed equations of state for neutron stars in the literature, though testing those equation-of-state models is, at present, very difficult due to the limitations of using telescope observations of neutron stars. Through detections of gravitational waves, scientists hope to be able to constrain neutron star equations-of-state. However, for the purpose of this project, we will assume an equation of state, since we do not yet have a confirmed detection of an NSBH system. For the purpose of our redshift calculation, we may use either the A18+dv+UIX model or the A18+UIX model from Akmal, Pandharipande, and Ravenhall (1998). Any choice of the neutron star equation of state presents biases in our mass, and therefore redshift, measurement.

• Calibration uncertainty - Feedback control of the gravitational wave interferometer introduces both statistical as well as systematic uncertainties into our measurement of gravitational wave strain. Initially, a combination of astrophysical strain and noise enter the interferometer, causing a differential arm length change, inducing the true detector response, which outputs a digital error signal in counts. That error signal is then converted back to strain through the modeled response function, resulting in a controlled arm length change, from which the feedback control process reconstructs the gravitational wave strain. Calibration of the interferometer is performed by shooting a photon calibration laser (of far lower frequency than the laser used in the interferometer) at the test masses, inducing their motion, and measuring it. The discrepancy between the true response function and the modeled response function is the source of calibration uncertainty in the interferometer (Cahillane et al., draft in progress).

Finally, we would like to propose ways of reducing these uncertainties and biases while performing cosmography with next generation gravitational wave detectors.

3 Description of Proposed Methods

Gravitational wave source are considered to be standard sirens due to the fact that their signals are well modeled, and we can determine the distance to the source using the signal amplitude. The distance to the source scales roughly inversely with the signal-to-noise ratio of the signal. Because we are interested in cosmography, we must consider the difference between the co-moving distance and the luminosity distance to a gravitational wave source. The luminosity distance is simply the co-moving distance multiplied by (1+z), and so is a function of the redshift of the source. Here, what we propose to measure directly from the signal-to-noise ratio is the source's luminosity distance.

3.1 Short GRB EM Counterpart method

For at least a small fraction of BNS mergers, we anticipate there to be an EM counterpart to the gravitational wave signal. The current working hypothesis is that BNS and NSBH systems are the progenitors for short GRBs. As shown by Metzger and Berger 2012, there are several different kinds of counterparts we can expect from a short GRB. Seconds after the merger, we could get gamma-ray emission from the GRB. Between hours to days surrounding a signal detection, we may observe optical emission from the GRB afterglow, as well as radio emission months after the signal is detected. While detecting a counterpart from the afterglow of the GRB may be challenging due to its dimness, the fact that the emission is detectable in longer wavelength bands for a longer timescale makes such coincident detections more plausible. The fact that jets from GRBs are beamed make them generally less likely to detect. However, the most promising counterpart for a BNS merger may be a kilonova, or the emission from the NS ejecta interacting with the surrounding gas and dust as the masses in the binary merge. This emission is predicted to be in the optical or the infrared (Metzger and Berger, 2012). One method of determining the redshifts of GW sources involves making a coincident GW-EM detection using large FOV telescopes, and following up the source with a spectrometer to obtain the source's redshift. We investigated the possible next generation telescopes that would a) have large enough FOV to be able to follow-up our BNS and NSBH detections, and b) have large aperture instruments capable of obtaining accurate source redshifts. A secondary method, involving localizing a source down to its host galaxy and using the galaxy's known redshift as the source's redshift would only involve using large FOV telescopes; however such a method would involve determining which galaxies are statistically favored as compared to others, as we anticipate there to be several galaxies within our localization regions in the next generation. Nevertheless, we include a table below with next generation telescopes that will survey galaxies as well as transients. The telescopes listed in the table below include the Large Synoptic Sky Survey Telescope (LSST), the Zwicky Transient Facility (ZTF), the Panoramic Survey Telescope and Rapid Response System (Pan-STARRS), the Dark Energy Camera (DECam), the Wide Field InfraRed Survey Telescope (WFIRST), the Wide Field Optical Survey (WFOS) telescope, as well as the Transient Astrophysics Probe X-Ray Telescope (TAP XRT). The next generation instruments we choose are not gamma-ray telescopes. In general, telescope observations in lower wavelength bands (x-ray and below) tend to have better localizations, which will allow us to more accurately obtain the source redshifts.

The degree of localization required for our gravitational-wave sources in the next generation is largely a function of the brightness of the source and the telescope field-of-view, and telescope aperture. If the source is below 24 mags in brightness, it is currently possible to search sky regions spanning 1000s of square degrees using wide FOV optical telescopes. However, to observe dimmer sources, or sources in lower wavelength bands, localizations of 100s or 10s of square degrees will be necessary in order to build a population of coincident GW-EM compact binaries, since larger aperture instruments will be capable of detecting dimmer

Table 1: Third Generation Telescope Parameters

Telescope	FOV (deg^2)	Sensitivity (mags)	Slew Time (s)	Mean Effective Aperture (m)	Wavelength Band (s)
LSST	9.62	25	5-12	8.4	optical
ZTF	47	20	15	1.2	optical
Pan-STARRS	7	30	10	1.8	optical
DECam	3	23	35	4	optical
WFIRST	0.281	26-27	68	2.4	infrared
WFOS	0.01	-	-	6.5-10	optical
TAP XRT	1	23-24	-	0.08	x-ray

sources, but may not have the capacity to search a wide sky region. LSST, which has both a large FOV as well as a large aperture appears to be our most promising telescope at present for third generation follow-up.

3.2 Tidal Disruption method

Gravitational wave signals provide an accurate measure of the chirp mass of the gravitational wave source, rather than the individual source component masses. The chirp mass is given by:

$$M_{chirp} = \frac{(m_1 m_2)^{3/5}}{(m_1 + m_2)^{1/5}} \tag{3}$$

which can also be re-expressed in terms of gravitational wave frequency. However, the measurement of the chirp mass from the signal is redshifted; for previous detections, we have assumed a given cosmological model (usually Friedmann-Robertson-Walker) and used the theorized values of H_0, Ω_Λ, Ω_M, and ω pertaining to that model, to determine the redshift of the binary black hole source from the distance formula given by equation two. Since the objective of cosmography is to determine how the distance relates to the measured redshift, in order to do cosmography using gravitational wave measurements alone, we require a way of breaking the mass-redshift degeneracy. A visible signature of the black hole disrupting a neutron star in a NSBH coalescence waveform would provide us precisely with that. By plotting the fourier transform of the NSBH gravitational waveform, one can determine the frequency at which tidal disruption occurs. We can re-express the frequency of gravitational waves in terms of the masses in the binary, using the fact that the gravitational wave frequency, $f_{GW} = 2f_{orb}$, the orbital frequency. Although in reality, the orbital frequency is derived from full general relativity, we can obtain a zeroth order approximation of it using Kepler's 3rd law and the relationship between the radius of innermost stable circular orbit (ISCO) of a black hole and its spin parameters. Here, we assume that the tidal disruption frequency is equivalent to the ISCO frequency of a black hole of mass equivalent to the total mass of the system. For such a black hole, from the Kerr metric, we obtain:

$$a_{ISCO} = \frac{6GM_{BH}}{c^2}(3 + Z_2 \mp \sqrt{(3 - Z_2)(3 + Z_1 + 2Z_2)}) \tag{4}$$

Here, $Z_1 = 1 + (1-\chi^2)^{1/3}[(1+\chi)^{1/3} + (1-\chi)^{1/3}]$, and $Z_2 = (3\chi^2 + Z_1^2)^{1/2}$, and χ is the dimensionless spin parameter J/M^2, where J is the angular momentum of the black hole, and M_{BH} is the black hole's mass. Then, $f_{orb} = 2\pi$ / T, where T is defined by Kepler's 3rd law as:

$$\frac{R^3}{T^2} = \frac{G(m_1 + m_2)}{4\pi^2} \tag{5}$$

and, replacing T with $1/f_{orb}^2$, we can write, in terms of the system parameters:

$$f_{orb}^2 = \frac{G(m_1 + m_2)}{4\pi a_{ISCO}^3} \tag{6}$$

Table 2: Initial Parameters of BNS and NSBH systems

$M_{1,NS}$	$M_{2,NS}$	$\chi_{1,NS}$	$\chi_{2,NS}$
1.2	1.4	0.00	0.00
1.2	1.4	0.05	0.05
1.4	1.4	0.00	0.00
1.4	1.4	0.05	0.05
1.6	1.2	0.00	0.00
1.6	1.2	0.05	0.05

$M_{1,NS}$	$M_{2,BH}$	$\chi_{1,NS}$	$\chi_{2,BH}$
1.2	7	0.05	0.99
1.2	7	0.00	0.00
1.4	12	0.05	0.99
1.4	12	0.00	0.00
1.6	14	0.05	0.99
1.6	14	0.00	0.00

But a_{ISCO} is a function of the spin parameters, so we can express the gravitational wave frequency, $f_{GW}^2 = 4 * f_{orb}^2$,in terms of the equivalent black hole mass and spin parameters, and some constants:

$$f_{GW} \approx \frac{c^3}{\sqrt{216\pi} G M_{BH}} (3 + Z_2 \mp \sqrt{(3 - Z_2)(3 + Z_1 + 2Z_2)})^{-3/2} \tag{7}$$

Since we are looking at tidal disruption, we recognize that the gravitational wave frequency is the same as the ISCO frequency, where tidal disruption occurs. Writing this more compactly in terms of $S(\chi)$, the dimensionless portion of the a_{ISCO} expression containing all of the spin parameters, we find:

$$f_{TD} \approx \frac{c^3}{\sqrt{216\pi} G M_{BH}} S(\chi)^{-3/2} \tag{8}$$

Of course, in order to find the true tidal disruption frequency of the system, or the ISCO frequency of the equivalent black hole, we need to perform the calculation in general relativity. Nevertheless, this method can be employed to find the zeroth order approximation for the way the ISCO frequency scales as a function of the total mass of the system. Identifying the frequency at which tidal disruption occurs will allow us to relate the mass that we measure, M_{chirp}(1+z) to the TD frequency we derived, and calculate the mass and redshift using a system of equations. Thereby, the main limiting factor to how well we can measure the redshift using this method is our ability to determine the TD frequency from the signal's fourier transform.

4 Waveform Visualization

In order to gain insight into how the component masses and spins affect gravitational waveforms of BNS and NSBH binaries, we simulated time domain waveforms of both types of systems using the lalsuite directory. For the BNS systems, we employed a SpinTaylorT4 approximant, and for the NSBH systems, we used the IMRPhenomB template approximant. We chose six different BNS and NSBH systems each, of which three of each type of system shared the same component masses, but had varied spins. We allowed our neutron star masses to range from 1.2-1.4M_{sun}, the spins to vary from 0.01-0.05, the black hole masses to vary from 7-14M_{sun}, and the spins vary from 0-0.99. Here, the spins are aligned and refer to the spin's z-component; the x- and y- components of the spin are assumed to be zero. Shown below is a table of the parameters we used for our six simulated BNS waveforms:

We examine systems of the same masses with minimal and maximal spin in order to clearly see the effect of spin on the BNS waveform. We plot h(t),the time domain strain data, the RMS signal amplitude in the time domain, as well as the amplitude spectral density in the frequency domain. We expect to observe a power-law relationship in the ASDs as a function of frequency in the BNS merger waveform. For a case with NSBH mergers, accurate waveform approximants will allow us to determine the frequency at which tidal disruption occurs, shown in the ASD of the NSBH merger. However, with the IMRPhenomB approximant we employed, we do not expect to see any tidal disruption signature in the ASD. The plots for the different scenarios are shown below.

What we observe is that for BNS mergers, the effect of spin in the time domain strain data for systems of the same mass with no spin and maximal spin is nearly negligible. The colored lines show gravitational waveform of BNS systems with maximal spin, and the dotted line indicates another system of the same

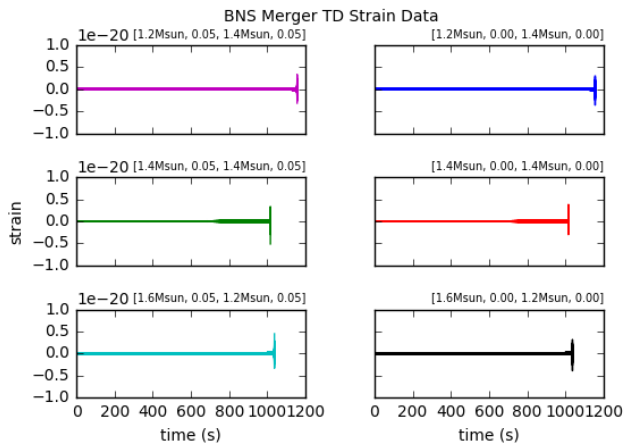

Figure 1: Time domain strain data for various BNS systems

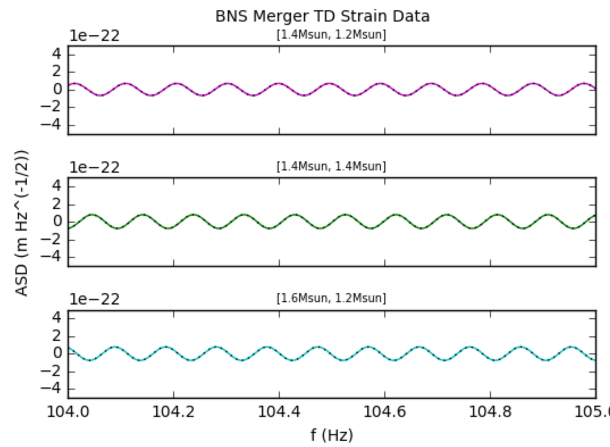

Figure 2: Zoomed in time domain strain data for various BNS systems

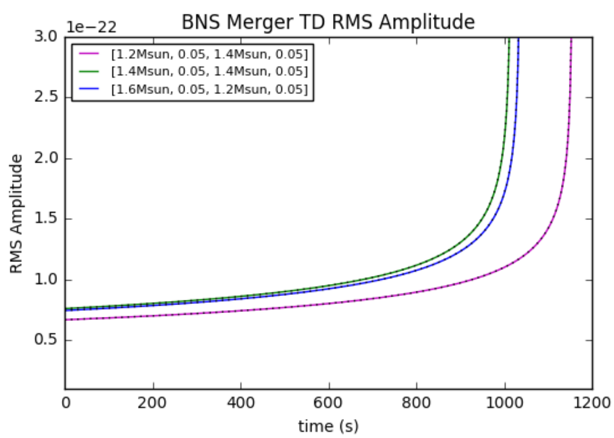

Figure 3: Time domain RMS amplitudes for various BNS systems

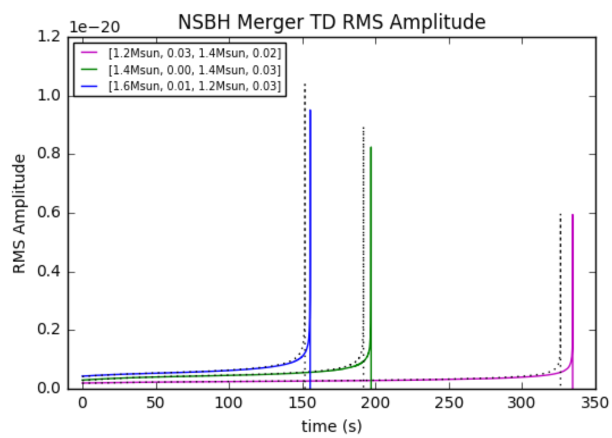

Figure 4: Time domain RMS amplitudes for various NSBH systems

mass but without spin. Similarly, when we plot the BNS RMS amplitude (constructed from adding the real components of the plus and cross-polarization strains to one another), it is clear from the fact that the dotted line plots directly on top of the solid colored line that the effect of spin is hardly perceptible. However, the plots suggest that more massive systems merge more quickly, and thereby in the RMS amplitude curves, the steep power-law behavior near the merger is shifted to the left for more massive systems.

Due to the fact that our waveform in the time domain is finite, we must examine its frequency-domain fast fourier transform (FFT) only in a limited range of frequencies. The FFT assumes that the input time-domain waveform continuously repeats itself for infinite time, which will not be the case. Thereby, we must be wary of edge-effects when analyzing our FFTs. Since we start our signal time domain waveforms from a minimum frequency of 10 Hz, we assume that the waveform is accurate above 20 Hz. In performing the FFT, we chose a sampling frequency of the power of two closest to twice the ISCO frequency, from the Nyquist sampling theorem ($f_{sample} = 2f_{max}$). Here, we take our maximum frequency to be the ISCO frequency, since the waveform approximants we use generally model up to the merger. Thereby, we can only trust the FFT data up to f_{ISCO}. In computing the FFTs, we faced a major challenge that the FFTs are computationally very costly to compute; our time-series data have a resolution of $\frac{1}{4096}$ s on average. We do not display the FFTs of these signals in the frequency-domain, but our next step will be to obtain the frequency domain strain data for each of these systems, as they are the most valuable component for identifying the tidal disruption

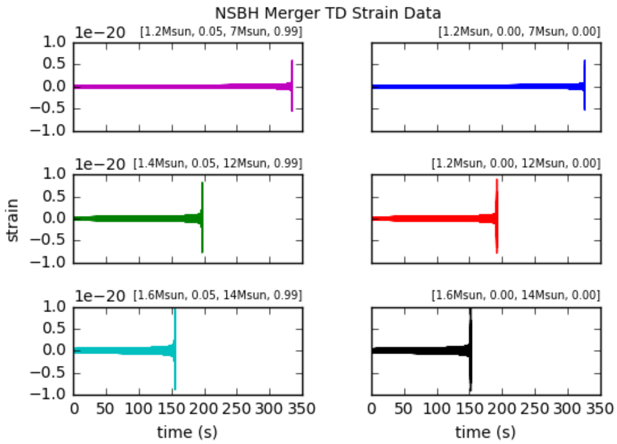

Figure 5: Time domain strain data for various NSBH systems

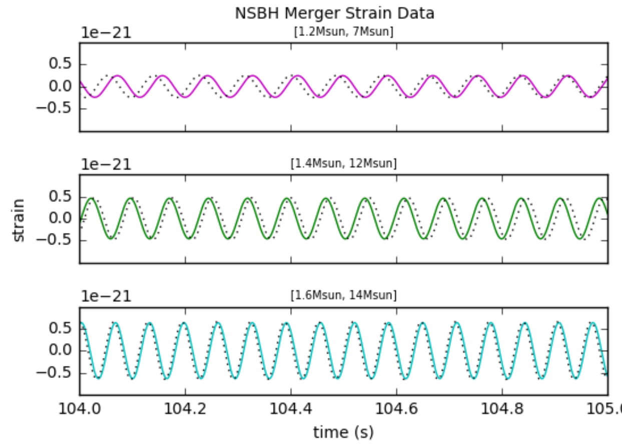

Figure 6: Zoomed in time domain strain data for various NSBH systems

frequency.

For NSBH systems, however, the change in the black hole spin creates a perceivable visual difference in the time domain strain data. We observe that a system with spin has a waveform that is phase-shifted with respect to the spin-less waveform; however the direction and amount of the shift is not the same in each scenario. It appears that systems that are less massive overall experience a larger phase shift with addition of spin.

This document is a record of our preliminary steps in gaining insight into the different aspects involved in our project. While we may not have made any significant progress towards our goal of measuring the systematic biases and quantifying the uncertainties involved in doing cosmography with gravitational waves, we have identified specific sources of error we are interested in further investigating, and hope to use these initial steps as a foundation to guide our project in the upcoming weeks.